PHILOSOPHICAL TRANSACTIONS A

Phil. Trans. R. Soc. A.
doi:10.1098/rsta.2018.0010

Melt Movement Through the Icelandic Crust

Robert S. White*, Marie Edmonds, John Maclennan, Tim Greenfield and Thorbjorg Agustsdottir

*Department of Earth Sciences, Cambridge University, Madingley Road, Cambridge CB3 0EZ, UK. *orcid.org/0000-0002-2972-397X*

Keywords: basaltic melt, Iceland, seismology, carbon dioxide, geobarometry, rifts

Summary

We use both seismology and geobarometry to investigate the movement of melt through the volcanic crust of Iceland. We have captured melt in the act of moving within or through a series of sills ranging from the upper mantle to the shallow crust by the clusters of small earthquakes it produces as it forces it way upward. The melt is injected not just beneath the central volcanoes, but also at discrete locations along the rift zones and above the centre of the underlying mantle plume. We suggest that the high strain rates required to produce seismicity at depths of 10 − 25 km in a normally ductile part of the Icelandic crust are linked to the exsolution of carbon dioxide from the basaltic melts. The seismicity and geobarometry provide complementary information on the way that the melt moves through the crust, stalling and fractionating, and often freezing in one or more melt lenses on its way upwards: the seismicity shows what is happening instantaneously today, while the geobarometry gives constraints averaged over longer timescales on the depths of residence in the crust of melts prior to their eruption.

Introduction

Almost all erupted melt is generated initially in the Earth's mantle. This melt usually interacts with the crust on its passage to the surface, and may reside in melt lenses, magma chambers or mush zones for long periods, of up to a few thousand years, before erupting [*Hawkesworth et al.,* 2000]. Of the primitive melt produced in the mantle, only a small fraction (typically estimated in the range of 5 − 20%) is erupted at the surface: the rest freezes in the crust or upper mantle. The primitive mantle melts are only rarely erupted: volcanic rocks are almost always the fractionated products of the primary melt. It is well known that fractionation occurs in the melt storage areas (usually called magma chambers) beneath active volcanoes, typically in the upper crust at depths of a few kilometres beneath the surface. However, petrologic evidence increasingly points to melt having also resided in deeper magma chambers, or more probably having passed through a series of stacked melt lenses, both in the crust and crust-mantle transition zone, and sometimes in the uppermost mantle on its passage to the surface [*Kelemen et al.,* 1997*; Stroncik et al.,* 2009*; Kiser et al.,* 2016].

*Author for correspondence (rsw1@cam.ac.uk).

In this paper, we discuss the evidence for melt moving through the thick Icelandic crust, which is 4 – 5 times thicker than normal oceanic crust, using both seismological and geochemical evidence. The advantage of constraints from microearthquakes is that they enable us to capture a snapshot of melt moving as it happens. Geochemistry provides depth constraints on a longer time-scale, recording depths at which melt has stalled and undergone some fractionation or chemical equilibrium. Iceland is particularly useful for mapping microearthquakes, because the brittle – ductile boundary under the neovolcanic zones that traverse Iceland occurs at a shallow depth of only 6 – 8 km below the surface. Brittle failure of the ductile crust does not occur under normal geological strain rates, so the ductile region is usually aseismic. However, if the ductile rock is subjected to sufficiently high strain rates it can sustain brittle failure, emitting seismic energy that can be detected at the surface as a microearthquake. Melt movement driven by increased magmatic or volatile pressure can provide locally high strain rates sufficient to promote brittle failure [*Wright & Klein,* 2006*; von Seggern et al.,* 2008*; Shelly and Hill,* 2011; *White et al.*, 2011; *Greenfield and White,* 2015]. Therefore, brittle failure microseismicity observed in the normally ductile and aseismic region of the Icelandic crust can be attributed to melt movement. We discuss deep crustal melt movement under four active volcanic systems: Bárðarbunga-Holuhraun, Eyjafjallajökull, Upptyppingar and Askja-Herðubreið. Each example provides insights into how the melt stalls, most likely in melt lenses that may freeze as sills, and moves through the crust. These examples show sub-vertical upward movement of melt, movement along a plane inclined at 50°, and 48 km of horizontal movement in a dyke prior to eruption.

Not all melt movement through the crust causes brittle failure that can be detected as micro-earthquakes. If melt percolates through the normal permeability of the crust it is likely to do so aseismically. In the mantle this is the normal method by which melt moves upward. The dihedral angle of mantle melts is less than 10° [*Cmiral et al.,* 1998] which allows all but a tiny fraction (estimated as a maximum of 0.5 – 1 % by volume) of the melt generated to drain efficiently from the mantle, driven by its buoyancy [*Zhu et al.,* 2011*; Laumonier et al.,* 2017]. If the crustal temperature is sufficiently high, then melt movement through channels may also occur aseismically; this may be the reason why much of the melt rising under active rift volcanoes produces little or no seismicity in the mid to lower crust directly beneath the volcanoes. It is more common to see deep seismicity caused by melt moving through cooler crust adjacent to the main volcanoes, as has been observed close to Askja [*Greenfield and White*, 2015] and Bárðarbunga [*Hudson et al.,* 2017] volcanoes. Ironically, we may detect more seismicity from the small volumes of melt moving upward through the cooler crust away from the main volcanic centres than we do from the large-volume melt feeders under the active volcanoes, because the crust containing large volumes of melt directly beneath active volcanoes makes brittle failure much less likely. In the case of the horizontal dyke which propagated from the Bárðarbunga volcano in 2014, despite over 31,000 earthquakes being recorded, they represent only 1% of the energy released by the rifting and dyking episode [*Ágústsdóttir et al.,* 2016]. Once a melt channel is open, the melt can flow aseismically.

Sometimes different types of earthquakes occur, also attributed to melt movement, known as ‘long period’ (LP) earthquakes. These contain lower frequency energy (typically 1 – 3 Hz) than the volcano-tectonic earthquakes discussed in this paper (which are typically 5 – 10 Hz). LP earthquakes have been reported from deep in the crust and in the upper mantle under Mammoth Lakes (USA) and Hawai’i [*Pitt et al,* 2002*; Okubo et al.* 2008]. These LPs are thought to be caused by fluid or gas resonance in a crack. We have found no evidence of LP earthquakes deeper than the upper crust in Iceland, although they do occur associated with melt in the upper crust [*Woods et al.,* 2018]. Their absence at depth is not surprising since special conditions of crack size and fluid content are necessary to produce LP earthquakes.

Iceland

The mid-Atlantic spreading ridge, where the separation of the North American and Eurasian plates leads to the formation of new oceanic crust, runs approximately north to south through Iceland. In addition, Iceland is also underlain by hot mantle, which is the expression of a deep sourced mantle plume [e.g. *White & McKenzie*, 1989; *White*, 1997; *French & Romanowicz*, 2015]. This causes dynamic uplift and leads to thickened igneous crust [*Darbyshire et al.*, 2000*; Jenkins et al.*, 2016, 2018], both of which mean that the active rift zone is elevated above sea level and therefore easily accessible for monitoring by seismometers and by geochemical and petrological sampling. Crustal formation occurring today along Iceland's volcanic rift zones is generated through the interplay of two geological processes: decompression melting occurring in the central rising stem of the mantle plume and decompression melting as a result of plate spreading. In order to resolve the trade-off between plume-driven melting and increased mantle temperature it is helpful to combine seismological constraints on crustal thickness with geochemistry [*Maclennan et al.*, 2001a].

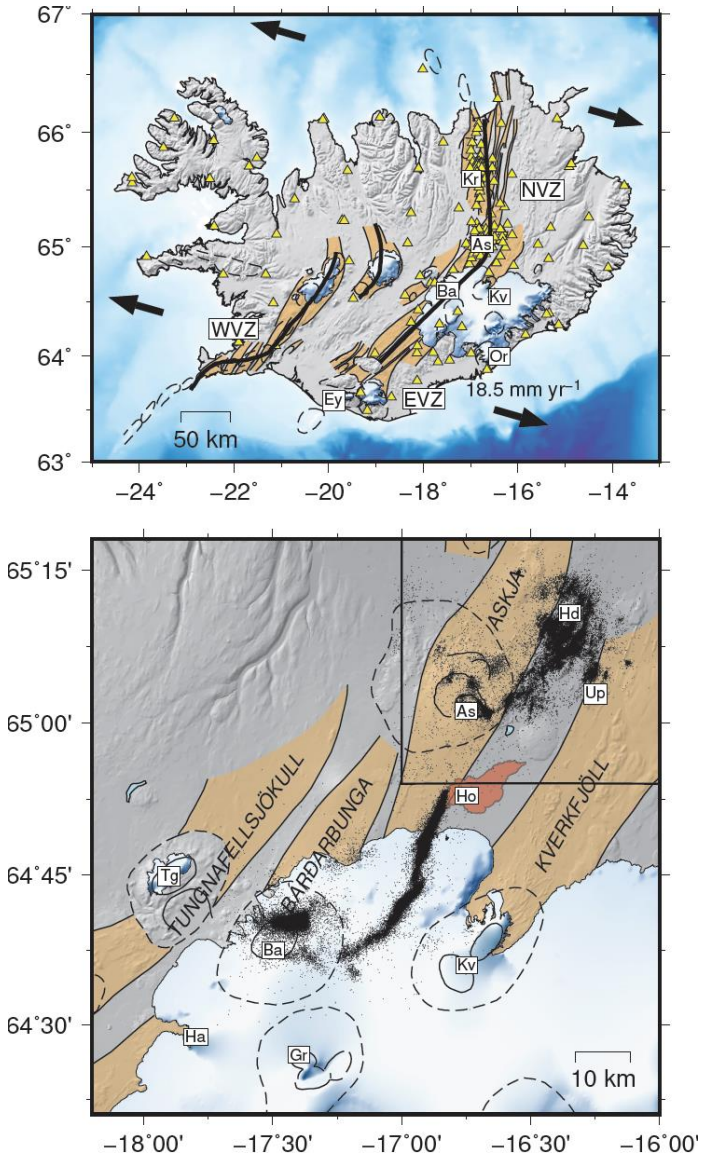

Figure 1. (top) Map of seismic stations (triangles) throughout Iceland with (bottom) enlargement of central region. Northern, Western and Eastern volcanic active rift zones are marked as NVZ, WVZ

and EVZ respectively. Plate spreading rate is from MORVEL [*DeMets et al.,* 2010]. *As, Askja; Ba, Bárðarbunga; Ey, Eyjafjallajökull; Gr, Grimsvötn; Ha, Hamarinn; Hd, Herðubreið; Ho, Holuhraun; Kr, Krafla; Kv, Kverkfjöll; Or, Öræfajökull; Tg, Tungnafellsjökull; Up, Upptyppingar.*

As it comes on land, the Mid-Atlantic spreading centre separates into three identifiable branches or neovolcanic zones, each containing the erupted products of recent magmatic activity: the Northern, Western and Eastern volcanic zones (NVZ, WVZ, EVZ, Figure 1). A ridge jump is currently in progress from the WVZ to the EVZ [*Hardarson et al.,* 1997]. Within the neovolcanic zones, the record of Holocene extension is mapped by the distribution of surface fractures and faults, which define distinct fissure swarms [*Einarsson & Sæmundsson,* 1987; *Hjartardóttir et al.,* 2009; *Hjartardóttir & Einarsson,* 2012]. These fissure swarms are each associated with a central volcano, and form the individual spreading segments of the rift (orange zones on Figure 1). The extension direction in Iceland is slightly oblique to the strike of the rift zones, at an azimuth of 106° at a full spreading rate of 18.5 mm/a [*DeMets et al.,* 2010], which is a relatively slow spreading ridge. However, the high magma supply at this hotspot creates greater crustal thicknesses than the ~ 7 km typical of normal oceanic crust spreading at the same rate [*White et al*., 1992]. Icelandic crustal thickness ranges from ~20 km near the northern and southern coasts to ~40 km beneath Vatnajökull, directly over the centre of the underlying mantle plume [*Darbyshire et al.,* 1998, 2000; *Jenkins et al.,* 2018]. There is a high geothermal gradient, which creates a brittle-ductile boundary at depths of 6 – 8 km over most of Iceland, with the deeper, hotter crust being normally aseismic.

No continuous axial melt lens is present, as is found for example at the East Pacific Rise, but several seismic studies of Icelandic central volcanoes have found evidence of significant shallow magma storage regions in the upper crust at depths of 3 – 6 km [*Einarsson,* 1978*; Brandsdóttir et al.,* 1992*; Gudmundsson et al.,* 1994*; Brandsdóttir et al.,* 1997*; Alfaro et al.,* 2007*; Schuler et al.,* 2015*; Greenfield et al.,* 2016].

Data

The main seismological constraints come from recordings acquired during dense deployments by the University of Cambridge of three-component broadband seismometers mainly in central Iceland, from 2006 to the present day. At its peak the number of seismometers deployed reached 75, but since they were moved around from time to time, and with the addition of data from some permanent monitoring stations run by the Icelandic Meteorological Office (IMO) plus other campaigns, data are available from 160 sites (Figure 1). Central Iceland provides a very quiet environment for recording microearthquakes, because there is no anthropogenic noise (e.g., wind turbines, cars, lorries, farming), and no noise from vegetation (tree roots are particularly noisy sources at seismic frequencies in windy weather). Additionally, during the winter the ground freezes hard, which provides good coupling of the seismometers to the ground, while the snow cover decouples the underlying ground from wind shear. Typically, we record microearthquakes down to magnitude 0, which means that we can detect tiny events even in the lower crust [*Greenfield et al., in press*]. All seismic data is recorded at 50 – 100 samples per second with a GPS timestamp. All the seismic hypocentres shown here are from locations made by Cambridge University. The sources of the geochemical data from the 2014 Holuhraun eruption, from the 2010 Eyjafjallajökull eruption and from the Askja rift are cited in the sections of the text where they are discussed.

Multiple Crustal Melt Feeders above the Rising Central Stem of the Iceland Mantle Plume

The rising central stem of the mantle plume sits beneath Vatnajökull ice cap (Figure 1). The diameter of the central stem where the crustal thickness is the greatest is of the order of 100 km [*Darbyshire et al.*, 1998; *Jenkins et al.* 2018]. There are at least six discrete volcanoes beneath and adjacent to the Vatnajökull ice cap, all of which have been active during historic times (Bárðarbunga, Grímsvötn, Hamarinn, Kverkfjöll, Öræfajökull, Tungnafellsjökull; see Figure 1).

Two main factors control the deep magma plumbing in this region. First, the melt is generated at depths > 40 km (i.e. below the crust), in the central rising region of the underlying mantle plume. Melting occurs as the convecting mantle rises and decompresses across the entire width of this central stem. But the initial feed of melt into the lower crust appears to occur at discrete locations, mainly beneath the active volcanoes. These multiple, transient feeder points into the overlying crust suggest that there is some focussing either in the upper mantle or at the crust-mantle boundary before the melt enters the crust. The main central volcanoes directly above the rising central part of the plume have remained active for at least 100,000 years. However, as noted in the next section, some melt also traverses the crust outside the main volcanoes. Second, the volcanic edifices themselves are likely to exert some control on the melt path near the surface, as the melt path is affected by the topographic loading of the volcanoes, by glacial loading, and by the influence of magma chambers [*Acocella and Neri*, 2003; *Karlstrom et al.*, 2009].

All the main volcanic centres under Vatnajökull have been seismically active since the area has been instrumented with seismometers (in the 1970s). Presumably they were equally active before instruments were available to record the earthquakes. This seismicity is generally constrained to the upper crust (less than 7 km deep), and is probably caused partly by tectonic faulting of the crust in the caldera above the main melt storage region and partly by geothermal activity in the shallow crust above the magma. When eruptions are imminent or melt is moving, this also causes seismicity, though usually only for the duration of the intrusion or eruption itself. Seismic precursors of Icelandic eruptions may last from minutes to days, though for half the 21 eruptions recorded since seismometers were used in the vicinity of active volcanoes, the precursor time was less than 2 hours [*Einarsson,* 2018].

Bárðarbunga: crustal melt feeds that bypass the volcanic caldera melt storage

Not all the melt traversing the crust accumulates directly beneath the volcanic calderas. One of the clearest examples is the deep sub-vertical column of crustal seismicity on the southeastern flank of the Bárðarbunga caldera shown in Figure 2. The deep seismicity, and hence melt plumbing, occurs primarily at depths of 7 − 22 km [*Hudson et al.,* 2017]. The lack of recorded seismicity below 22 km does not mean there is no melt transport there, since melt must travel up from its source in the mantle below this depth. It may be that the crust is hotter and more ductile at greater depths, requiring higher strain rates for fracture, with insufficient fluid pressures to drive this. Indeed, it is likely that melt also ponds as lenses in the upper mantle and in the crust-mantle transition zone. This sub-vertical column of seismicity was active several years before the 2014 – 15 Bardarbunga – Holuhraun eruption, and has continued subsequently to the present day, with little change in the frequency of earthquakes [*Hudson et al.,* 2017]. So this vertical melt feeder does not appear to be related directly to the onset of the dyke propagation discussed below.

Although crust-cutting seismic activity is confined to the southeast outer flank of Bárðarbunga, this lateral offset is not an unusual observation [*White and McCausland*, 2016]. Other volcanoes such as Askja (discussed later) [*Greenfield and White*, 2015], Kīlauea (Hawai'i) [*Wright and Klein*, 2006; *Bell and Kilburn*, 2012; *Wech and Thelen*, 2015; *Lin and Okubo*, 2016], Mount St Helens (US) [*Kiser et al.*, 2016] and El Hierro (Canary Islands) [*Klügel et al.*, 2015] also have deep seismicity with similar lateral offsets from the associated volcanoes. Bárðarbunga's main magma storage region is thought to be at 5 – 12 km depth bsl [*Gudmundsson et al.*, 2016*; Ágústsdóttir et al., in review*]. However, Ágústsdóttir et al. (2018) and Hudson et al. (2017) find only a handful of events deeper than 8 km under the caldera.

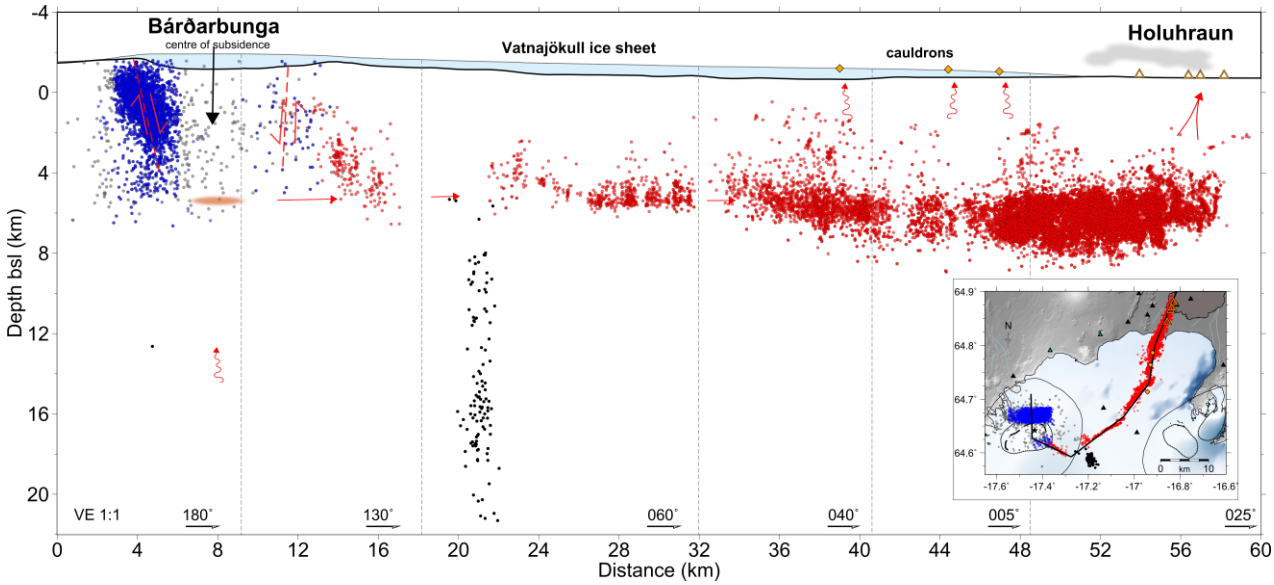

Figure 2 *Stitched-cross-section at true scale summarising seismicity during the 2014 – 2015 Bárðarbunga – Holuhraun eruption. Caldera earthquakes in blue and dyke intrusion earthquakes in red. Black are events observed from 2012 – 2017 in the persistent narrow deep seismicity cluster outside the caldera from Hudson et al. [2017]. Orange diamonds show ice cauldrons formed during the eruptive period. Glacier topography shown in light blue and bedrock with black line* [*Björnsson & Einarsson*, 1990]. *Red arrows show melt flow constrained by the seismicity, squiggly red arrows show inferred melt pathways. Red dashed lines are inward dipping caldera faults with associated slip direction. Vertical grey lines show projection segments of the stitched-cross-section. Inset map: thick black lines show the segments of the stitched-cross-section. Triangles show seismometer sites.*

In some other volcanoes, there is also evidence from petrological constraints of laterally offset melt plumbing that leads to magma bypassing the main caldera melt source. For example, the lavas erupted to the north of the Krafla caldera during the 1975 − 1984 rifting episode exhibit marked petrological and geochemical differences from those lavas erupted within the caldera, suggesting that they bypassed the magma reservoir under the caldera [*Grönvold et al.*, 2008]. Likewise, in the hotspot volcano of Kīlauea, primitive magmas may bypass the summit storage region on their way to eruption sites on the upper rift zones [*Vinet and Higgins*, 2010; *Sides et al.*, 2014*; Helz et al.*, 2015]. Our seismic results from Bárðarbunga capture an instance of some melt bypassing the main caldera storage region.

Bárðarbunga - Holuhraun: sub-horizontal melt transport

A 48 km dyke was intruded north-east from Bárðarbunga volcano to a distant eruption site at Holuhraun in 2014, feeding a 6 months long eruption, and providing an example of melt flowing sub-horizontally a long distance along a volcanic rift (Figure 2). Sub-horizontal flow occurs frequently in the Icelandic rift zones: other recent examples include the Krafla eruptions in the 1980s [*Einarsson & Brandsdóttir,* 1978], the subglacial Gjálp eruption between Bárðarbunga and Grímsvötn in 1996 [*Einarsson et al.,* 1997], and the Askja eruption in 1875 [*Sigurdsson & Sparks,* 1978*; Hartley & Thordarson,,* 2012]. A detailed study of more than 31,000 earthquakes produced during the two-week long lateral dyke propagation from Bárðarbunga shows that the melt travelled at 6 – 7 km bsl. The forward propagation was episodic, in bursts of forward motion at speeds varying from 0.3 – 4.7 km/hr over distances of 2 – 4 km, interspersed with periods of typically tens of hours as the dyke stalled [*Ágústsdóttir et al.,* 2016]. The path taken by the melt was along the direction of least lithostatic pressure [*Sigmundsson et al.,* 2015], with the initial eruption utilising exactly the same cones in Holuhraun as had been active in an earlier eighteenth or nineteenth century eruption [*Hartley et al.,* 2018]. This shows that melt paths through the crust may be re-occupied by melt feeding subsequent eruptions.

The Bárðarbunga – Holuhraun dyke was accompanied by up to 4 m of opening recorded by GPS on either side of the rift [*Sigmundson et al.,* 2015]. From this we can calculate the total moment release to compare with the seismic moment release calculated by summing that from each earthquake. Only 1% of the geodetic moment release was recorded seismically by the 31,000 earthquakes. The earthquakes only record the cracking of the rock near the tip of the dyke, and induced seismicity adjacent to it, whereas the subsequent opening of the dyke and magma flow along it are aseismic [*Ágústsdóttir et al.,* 2016]. This provides a good reminder that the earthquakes are indicative of where melt is opening a new subsurface channel, but they do not generally give direct information on melt flow.

Petrological studies of the Holuhraun lava flow also provide some constraint on the location of magma storage in this system. OPAM barometry is based upon a parameterisation of the composition of experimental liquids that are known to be in equilibrium with olivine, plagioclase and clinopyroxene crystals [*Yang et al.,* 1996]. This barometer can be applied to any liquid composition, but only provides meaningful results for tholeiitic basalts that are demonstrably in equilibrium with these three solid phases. Holuhraun tephra is composed of a basaltic glass that is a quenched version of the liquid that travelled upwards from the melt storage regions. In this case, as for most relatively water-poor basalts, very little crystallization appears to have taken place in a magmatic conduit because clean, fresh glass-dominated tephra is available. The carrier liquid did, however, transport crystals from storage zones in the Bárðarbunga plumbing system. The rims of these olivine, clinopyroxene and plagioclase crystals appear to be in textural and chemical equilibrium with the carrier liquid, indicating that the OPAM method may be appropriate in this case.

A new application of the OPAM parameterisation by *Hartley et al*. (2018) found that the Holuhraun melt was stored at 2.1 +/- 0.7 kbar, equivalent to a depth of about 7.5 km below the surface. Another barometer, which relies upon the exchange of sodium between clinopyroxene and liquid, was also applied to the products of this eruption [*Neave & Putirka,* 2017; *Halldórsson et al*., 2018] and found that the clinopyroxenes equilibrated with the carrier liquid at the same pressure of 2.1 +/- 1.5 kbar. The close correspondence in pressures between the two barometers indicates strongly that the final depth of storage and equilibration of the Holuhraun magma was close to 7.5 km depth (~ 6 km bsl),

similar to the cut-off depth of seismicity beneath Bárðarbunga (Figure 2), which therefore indicates the depth of the main magma chamber.

A history of deeper melt storage is recorded within the cores of the crystals that were brought to the surface during the Holuhraun eruption. Clinopyroxene-liquid equilibrium indicates that a subset of the crystals were carried from pressures of 3 kbar or more [*Halldórsson et al*., 2018]. OPAM barometry on corrected melt inclusion compositions from these more primitive crystals also provides pressures of 3.2 kbar [*Hartley et al*., 2018]. Dense, CO_2-dominated fluid inclusions found in these crystals appear to have been trapped at pressures of as much as 4 kbar [*Bali et al*., 2018]. It is clear that crystals formed in deep storage zones, at 15 − 20 km depth, were carried into a shallower storage zone in the Bárðarbunga system. This pressure range may be related to the observed depth range of seismicity in the plumbing system. It is not yet possible, however, to link these deeper-formed crystals to a specific lateral position of storage, nor to constrain the timescale between their crystallization at depth and their entrainment for eruption. So we cannot at present tell whether the entrained crystals came from directly beneath the Bárðarbunga caldera or from the deep feeder outside the caldera.

Eyjafjallajökull: release of melt from successively deeper sills during eruption

Eyjafjallajökull volcano lies near the southern end of the EVZ, where the active rift zone is propagating southwards (Figure 1). In 2010 it erupted first with a small (0.02 km^3) mafic flank eruption at Fimmvörðuháls which lasted 3 weeks, then after a two-day hiatus, an explosive eruption occurred at the summit caldera, which lasted over a month. The latter eruption was sub-glacial, and created an ash plume which spread over northwest Europe and disrupted over 100,000 airplane flights. These eruptions were preceded by 16 years of unrest recorded seismically and geodetically, including crustal intrusions of melt lenses without eruptions recorded in 1994, 1996 and 2009. Seismicity associated with the 1996 intrusion was close to the base of the crust at depths of 20 – 25 km [*Hjaltardóttir et al.*, 2009]. These melt lens intrusions were followed by a much more intense period of seismicity at depth in December 2009, which continued and intensified until the flank eruption began in March 2010 [*Sigmundsson et al.*, 2010] (Figure 3a). The magmatic intrusion causing most of the seismicity was likely to be a laterally inflating complex of sills at about 4 km depth, with seismogenic pinch-points occurring between aseismic compartments of the sills, or between adjacent magma lobes as they inflated [*Tarasewicz et al.*, 2014]. During the final four days before the top crater eruption started, the seismicity shallowed upward to a depth of about 2 km [*Tarasewicz et al.*, 2014].

Geobarometric constraints suggest that the flank magma was partially crystallized at 16 – 18 km depth [*Keiding & Sigmarsson*, 2012], consistent with the seismic observations. Application of the more recent parameterisation of clinopyroxene-liquid equilibrium by *Neave & Putirka* (2017) to these data also recovers an equilibration pressure of 4 – 6 kbar (12 – 18 km below the surface), which is consistent with lower-crustal pre-eruptive storage in this system. While *Keiding & Sigmarsson* (2012) recovered OPAM equilibration pressures of 6.4 kbar from the Fimmvörðuháls tephra glasses, careful application of the updated OPAM parameterisation described in *Hartley et al.* (2018) gives very low pressures of final equilibration, of < 0.5 kbar (1.5 km below the surface). Clinopyroxene-liquid equilibrium from the summit eruption material provides a large range of pressure estimates, generally shallower than those derived from the flank-erupted material. These findings indicate that application of the barometers to the unusually Ti, Na and K-rich basalts of the Eyjafjallajökull system provides challenges for parameterisations that are calibrated for standard tholeiitic systems.

The main eruption from the central Eyjafjallajökull caldera started on 14 April 2010, when mafic melts intercepted a shallow chamber containing evolved silicic melts, which were then destabilised (Figure 3b). A little over two weeks later, a series of successively deeper swarms of seismic activity were recorded. These have been interpreted as being caused by the release of melt from melt lenses at several different depths in the mid and lower crust and the upper mantle (Figures 3c,d) [*Tarasewicz et al.*, 2012]. As the uppermost magma chamber and the ice covered caldera lost mass by lava flows, expulsion of ash plumes and melting of the ice load, the pressure in the underlying crust would have dropped. By far the biggest loss of mass was the expulsion of fine tephra, which amounted to 0.27 km^3 (bulk volume) and which removed the mass far away from the volcano. In contrast, the lava flows totalled an order of magnitude less, at 0.027 km^3. If the melt in the crustal lenses were sitting close to lithostatic pressure, then this decrease in the overlying pressure could have been sufficient to allow the melt to break out of the lens and move up the open conduit toward the surface. This process would then repeat and propagate downwards as each successive lens lost melt. This is an intriguing observation, because it suggests that a considerable quantity of melt was stored simultaneously in lenses at several different depths in the crust, and indeed also in the uppermost mantle. These seismological observations are consistent with petrological and geochemical inferences of depths of residence of melt in the crust.

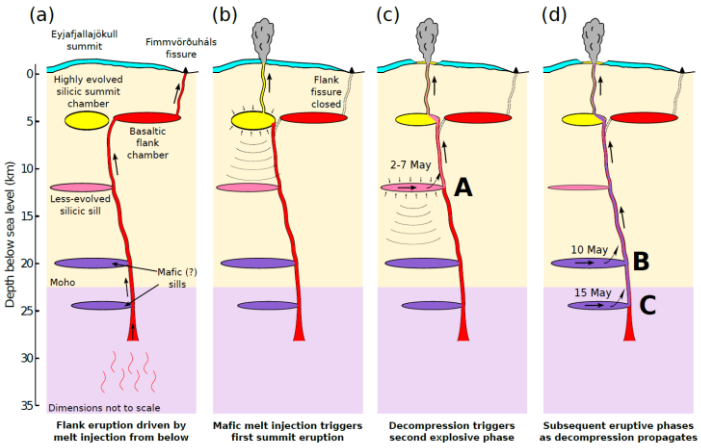

Figure 3. *Cartoon illustrating melt sources during eruption under Eyjafjallajökull in 2010 (from Tarasewicz et al., 2012). (a) Fimmvörðuháls flank eruption. During January–March 2010, low-viscosity, mafic melt flows up conduit from depth and inflates the eastern volcano flank, without extensive mixing with deeper sills. Fissure eruption of alkali basalt starts 20 March. Mafic melt continues to flow into flank chamber; no deflation observed geodetically [Sigmundsson et al., 2010]. (b) Fissure eruption ends 12 April. Summit eruption starts 14 April, triggered by mafic melt injecting into evolved silicic melt in magma chamber beneath summit crater [Sigmarsson et al., 2011]. Explosive activity subsides into effusive lava eruption. (c) Depressurization of shallow summit chamber causes melt mobilization at 10–15 km depth starting 2 May. Resurgence in explosive activity on 5 May incorporates melt from sill at 10–15 km depth and fresh, primitive melt residing in the conduit. (d) Subsequent decompression wave mobilizes melt at ~19 km (10 May), and then ~24 km depth (15 May), causing seismic swarms as melt escapes from sills. Eruptions follow each burst of deep seismicity, lagging by 1–3 days. Eruption dies down as mafic melt supply reduces and overpressure is relieved.*

Upptyppingar: intrusion without eruption

The Upptyppingar unrest provides a seismically well-monitored example of melt intrusion into the mid-crust which then stalled without erupting. As mentioned earlier, most of the melt intruded into the crust does not erupt, but eventually freezes within the crust, as this intrusion did. Mount Upptyppingar lies north of the Vatnajökull ice cap (Figure 1), and the intrusion occurred over a period of one year starting in March 2007, producing over 10,000 located microearthquakes. The 0.05 km^3 intrusion occurred along a dyke which reached a maximum thickness of ~1 m, dipping southwards at 50°, as melt moved upward from a sill at ~18 km depth to the shallowest level of intrusion at 13.5 km (Figure 4), and with a lateral extent of ~ 5 km [*White et al.,* 2011]. The 50° inclination is unusual, since melt usually intrudes either horizontally as sills or sub-vertically as dykes (and sometimes the nomenclature 'sheets' is used for inclined melt intrusions such as this). However, in this case, the inclination is likely to be due to its location north of the Vatnajökull ice cap: melting of the ice cap is causing isostatic uplift at a rate of ~20 mm/a, which is similar to the spreading rate of the rift, thus creating a stress field which may favour inclined injection of sheets [*Hooper et al.,* 2011].

We learn several important things from this dyke. First, the seismicity occurs in local swarms usually lasting several hours but separated by quiescent periods lasting from tens to hundreds of hours. If the seismicity is tracking the episodic melt movement, then the rate of melt movement is typically 2 – 3 m/min. Second, the well-constrained fault plane solutions have fault planes with dips and strikes that align precisely with the macroscopic dip of the dyke (Figure 4). Although popular models of dyke injection suggest that fractures ahead of a dyke tip should be orientated at angles of around 30° to the direction of dyke propagation [*Rubin & Gillard*, 1998], that is not the case here. Third, both normal and reverse faulting occurs, all with the same alignment of planes parallel to the dyke. Sometimes normal and reverse faults occur within minutes of each other, in locations that are identical to within our resolution [*White et al.,* 2011]. This suggests that these rapidly reversed faults may be occurring within fragments of frozen melt in the dyke. In this relatively thin dyke (estimated as 0.15 – 0.2 m thick), melt intruded at a temperature of 250°C above the country rock temperature will freeze within a few hours. Even a dyke 1 m thick would freeze within a day or two [*White et al.,* 2011]. When melt cools from a high temperature, its shear modulus initially increases as it goes through a glass transition, but once it cools below a homologous temperature of about 0.7 it undergoes shear weakening due to the growth of microcracks or stress-induced crystal growth [*White et al.,* 2012]. So it may be that melt frozen in constrictions in the dyke is repeatedly fractured by the pressure of rising melt, with either normal or reverse faulting occurring, depending on which side of the melt plug is broken (see *White et al.,* 2011 for further details). Each fracture would create a small microseism. It is also possible that the faulting is in the country rock immediately adjacent to the dyke, because such faults sub-parallel to dykes have been reported from outcrops elsewhere [*Kavanagh et al.,* 2011].

This dyke injection also yielded another important insight. A burst of seismicity directly above the dyke started at the brittle-ductile boundary a few months after the dyke had stalled. If, as we believe, the melt movement was triggered by the release of volatiles, and in particular of CO_2, then it is possible that after the melt stopped moving upwards the CO_2 continued to percolate up, then triggered pre-existing weaknesses near the base of the brittle crust by reducing the normal stress on the fault planes. *Martens & White* (2013) estimated the Coulomb stress on the faults near the brittle-ductile boundary which was generated by the dyke expansion as 200 kPa (2 bars). Since the elastic response which generated the Coulomb stress was imposed immediately as the dyke was emplaced, it required several months for the CO_2 to percolate up so as to enable the faults to break. This requires a hydraulic diffusivity of 1.0 – 3.3 m^2/s in the 6 km of crust between the top of the dyke and the new faults. Faulting continued at the brittle-ductile boundary for 4 years, but the rate of seismicity

decreased over that time. The reducing level of activity with time following the intrusion is consistent with both depletion of the carbon dioxide source at depth following the termination of the magmatic intrusion as well as having triggered many of the faults that were already primed and close to failure.

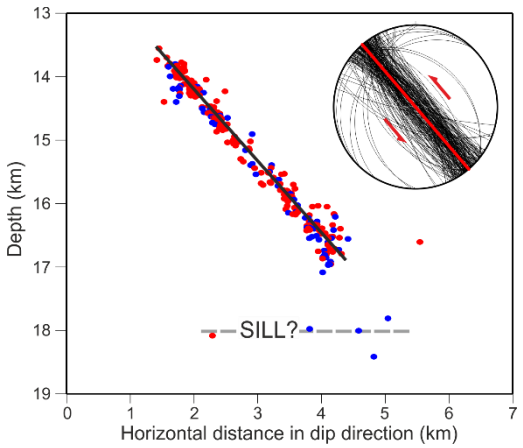

Figure 4. *Vertical cross-section at true scale looking along strike of Upptyppingar dyke during the 6–24 July 2007 period of melt injection (from White et al., 2011). Dots show earthquakes with fault plane solutions controlled by 12 or more polarity picks: red are reverse faults, blue are normal faults. Inset shows fault planes from 229 double couple reverse solutions viewed along strike and projected onto an equal area projection orientated vertically and orthogonal to the dyke. Broken grey line shows speculative location of a feeder sill.*

Askja Rift: intrusion beneath and adjacent to the caldera with multiple sills at depth

The most recent caldera-forming eruption in Askja volcano (see Figure 1 for location) was in 1875. It was accompanied by eruptions along the volcanic segment to the north of Askja, suggesting that there was also significant lateral flow of magma along the rift similar to that discussed above for the 2014 Bárðarbunga eruption [*Hartley & Thordarson*, 2012]. A series of smaller eruptions around the caldera followed, with the most recent eruption in 1961 when a 2 km long fissure opened on the north side of the volcano and erupted for 5 weeks [*Thorarinsson*, 1962]. Persistent seismicity, geothermal activity, reduced seismic velocities (especially of shear waves, Vs) and geodetic measurements over the volcano suggest that there is still a large quantity of magma present beneath Askja.

The magmatic plumbing system beneath Askja has been imaged using local earthquake tomography [*Greenfield & White*, 2016]. There is a series of high-Vp/Vs ratio bodies indicative of the presence of melt situated at discrete locations throughout the crust to depths of over 20 km (Figure 5). The main melt storage regions lie directly beneath Askja volcano, concentrated at depths of 6 km below sea level (bsl) with smaller regions at 9 km bsl. Their total volume is ~100 km^3. Seismic attenuation of waveforms suggest that here is also likely to be a small, highly attenuating magmatic body at a shallower depth of about 2 km bsl, which is consistent with interpretations from geodetic studies [*de Zeeuw-van Dalfsen et al.*, 2012].

The main seismic anomaly at 6 km depth bsl (oval black line, Figure 5) is unlikely to be pure melt because shear waves pass through this region. The resolution of the seismic tomography cannot

distinguish between multiple small melt lenses containing melt intruded into the crust and a broader volume of mush. Over the volume shown by the black oval, *Greenfield & White* [2016] use the measured Vp and Vs values to estimate the average melt fraction as ~10%. There is no seismicity within this volume, which also points to the likelihood of it being at a high temperature that is unable to support brittle fracture [*Greenfield & White*, 2016]. It is likely that this melt storage region was formed initially by the intrusion of sills, possibly by the deflection of dykes at a rheological boundary [*Kavanagh et al.*, 2015]. Once intruded, the sills could act as a locus for successive rising dykes, thereby creating a heavily-intruded region of the crust [*Menand*, 2011], or mush zone.

In the lower crust there are clusters of seismicity at depths of ~15 and 20 km beneath the caldera, although they are located beneath the edge of the caldera rather than directly under it's centre. Small regions of lowered seismic velocity are associated with them, but the anomalies are much smaller than in the shallower crust, which is probably why we are able to detect seismicity within them. As discussed in an earlier section, the very fact that there is seismicity here suggests that melt is moving within or through these regions.

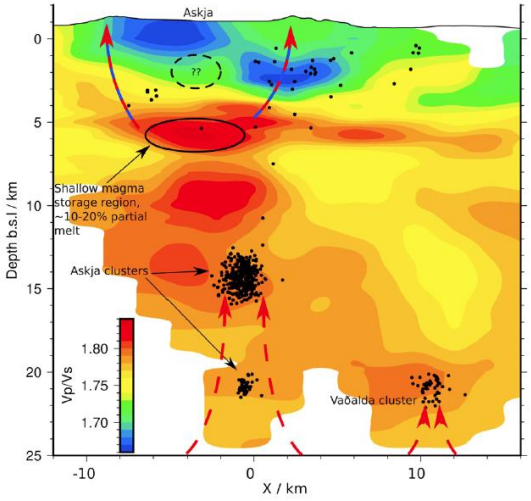

Figure 5. *Interpretation of the velocity structure and seismicity parallel to the plate spreading direction beneath Askja volcano (cross-section location shown on Figure 6) from Greenfield & White* (2016). *The section is plotted through the Vp/Vs model which is sensitive to the presence of melt. Seismicity within 2 km of the profile is shown by the black dots. The imaged magma storage body in the upper crust is outlined by the solid black line, with the maximum possible size of any shallow low-velocity body centred at 2 km depth indicated by the dashed black oval. Dashed red lines show the interpreted flow of melt through the crust.*

In addition to the evidence for melt beneath Askja volcano itself, there are also several locations of persistent seismicity in the mid and lower crust along the neovolcanic zone associated with Askja (orange dots, Figure 6). These have been known to be active for over a decade, ever since there have been seismometers in the area capable of recording them. The earthquakes occur in swarms of near-identical repeating events sometimes as close as 8 seconds apart, lasting for up to 3 hours [*Greenfield & White*, 2015]. They are small events with magnitudes ranging from -0.5 to 0.4 (note that the magnitude scale is logarithmic, so a magnitude -0.5 earthquake has ten times smaller amplitude than a magnitude 0.5 earthquake, and emits about 30 times less energy). Moment tensor solutions show that most of the earthquakes are high-angle opening cracks accompanied by volumetric increases. This is consistent with the failure causing the earthquakes being melt injection opening new tensile

cracks. The cracks are likely to form at the tips of sills, where stresses are highest. Earthquake locations from high-resolution mapping show that although individual swarms have dimensions of < 100 m, they are spread across regions about 1 – 2 km across. So it is likely that we are imaging melt moving between smaller lenses or melt pockets embedded in a locally heavily intruded region.

This is another example, like Bárðarbunga, of melt in the deep crust outside the main central volcano of the neovolcanic rift segment. It is likely that this seismicity represents smaller amounts of melt than reside under the central volcano itself, but it suggests that not all the melt is focused under the central volcano. Unlike the Bárðarbunga example, we do not see a vertical string of seismicity from the deep to the shallow crust, so we cannot tell whether the melt represented by the deep seismicity we record along the Askja rift is caused by melt rising from the mantle, or whether it was emplaced by horizontal flow from the central volcano. Both are possible, and indeed likely.

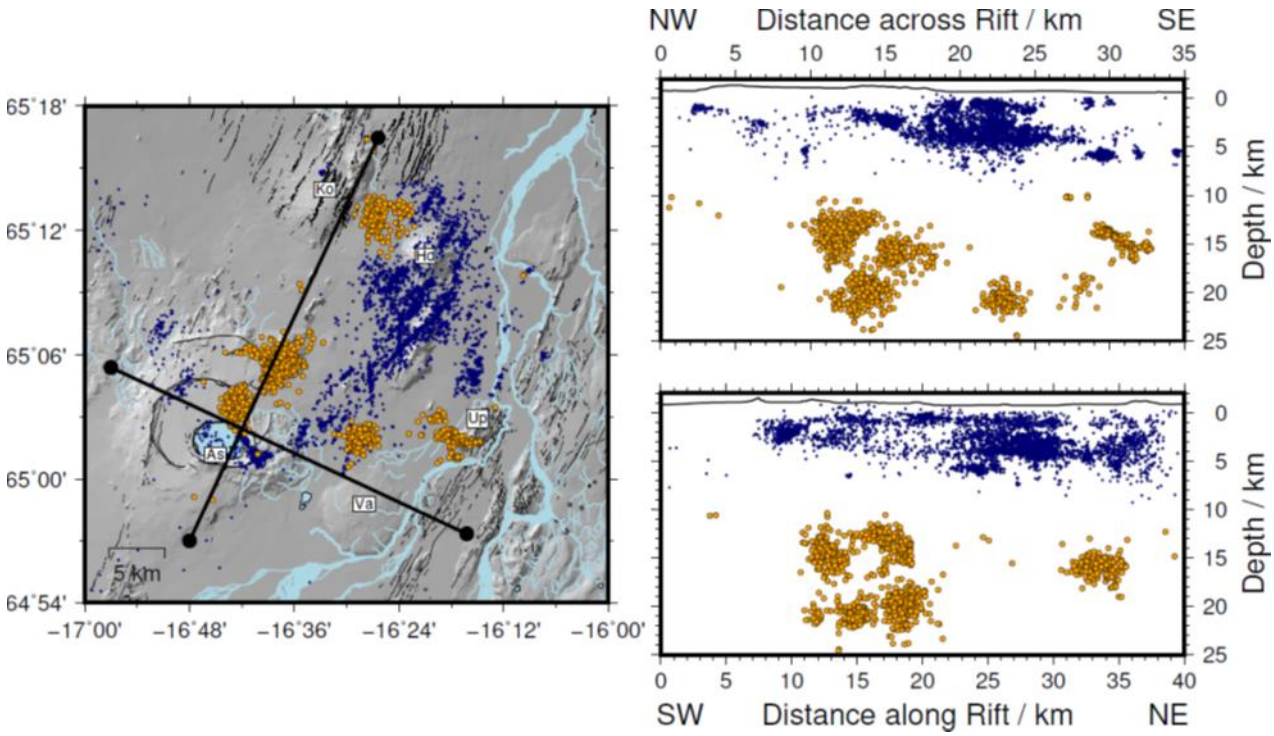

Figure 6. Seismicity in the Askja neovolcanic rift from 2006 −2015 (modified from Greenfield & White 2015). Blue earthquakes are in the brittle upper crust, orange earthquakes in the normally ductile lower crust. Map shows locations of the cross-sections displayed on the right. Profile shown in Figure 5 is along NW – SE line. As, Askja; Hd, Herðubreið; Ko, Kóllottadyngja; Up, Upptyppingar; Va, Vaðalda.

The results of petrological investigation of the Askja system by *Hartley & Thordarson* (2013) can be compared with the detailed seismological findings. These authors found a large range of clinopyroxene-liquid equilibration depths, but with a mean of significant basaltic eruptions from the last two centuries at 2 – 3 kbar (6 – 9 km bsl). Application of the new parameterisation of the OPAM barometer to the melt data from *Hartley & Thordarson* (2013) provides a mean equilibration pressure of ~2 kbar. These pressures correspond to those of the depth of the large Vp/Vs anomaly found at ~ 6 km bsl under the Askja central volcano. A handful of samples from small, intra-caldera eruptions of the 20th century provide clinopyroxene-liquid equilibration pressure estimates of < 2 kbar. A

petrological record of magmatic storage in the lower crust is not yet available from the Askja system, but will be the target of future studies.

Multiple crustal sills

As discussed above, there is strong evidence from Iceland that the melt rising from the mantle stalls at intermediary sills on its way to the surface, consistent with the stacked-sills model of crustal accretion for Iceland proposed by *Maclennan et al.* (2001b) on the basis of clinopyroxene-liquid and OPAM barometry. This is in agreement with previous work in Iceland by *Pálmason* [1971] and *Brandsdóttir et al.* [1997] which suggests that melt plumbing characteristic of large Icelandic central volcanoes is likely to comprise a complex network of lateral sills beneath each volcano, with magma rising within high density intrusive complexes near the surface. Seismicity from the Askja region, Bárðarbunga, Upptyppingar and Eyjafjallajökull shows that active melt movement can be seen down through the entire crust and into the upper mantle. Surface eruptions may tap melt from one or more of these sills, although the main eruptions from the central volcanoes that are associated with each neovolcanic rift zone generally erupt magma which has accumulated at shallow depths of 3 – 6 km under the volcanoes [*Einarsson* 1978*; Brandsdóttir et al.,* 1992*; Gudmundsson et al.,* 1994*; Brandsdóttir et al.,* 1997*; Alfaro et al.,* 2007*; Schuler et al.,* 2015*; Greenfield et al.,* 2016]. In the sills at 20 km depth near Askja, there is evidence of melt moving locally between smaller pockets spread across a region of the order of a kilometre or two across, causing repeated bursts of seismicity: this may be an example of multiple small sills at a similar depth, or of pockets of melt remaining within a larger, cooling sill.

Direct observations of igneous sills intruding the lower crust come from seismic reflection profiles across highly stretched crust on the early Tertiary continent-ocean boundary near the Faroe Islands in the North Atlantic [*White et al.*, 2008]. This is an analogue of the current rift under Iceland because it was generated by stretching above a mantle plume. On the continental margin the intrusive igneous sills have much higher seismic velocities than the continental country rock they are intruding, so they create large impedance contrasts which can be imaged on reflection profiles. There are no comparable deep penetrating seismic reflection profiles across the active Icelandic rifts, and in any case they would probably not show such clear reflections because the sills are intruding material of the same igneous composition. However, the presence of fractionated igneous rock (and therefore of melt residence for some time) in the lower crust may be inferred because receiver function and seismic refraction studies show a high seismic velocity of the lower Icelandic crust in crust deeper than 20 km which is probably due to ultramafic cumulates, possibly intermixed with gabbroic rocks that are left behind after fractionated melt moves to shallower levels [*Jenkins et al*, 2018].

The role of Exsolved Magmatic Carbon Dioxide in Inducing Seismicity

The occurrence of frequent microearthquakes in the normally ductile middle and lower crust of Iceland under the neovolcanic rift zones must reflect locally high strain rates in order to produce brittle failure. The most likely cause is the movement of melt or other fluids which can produce high strain rates. In addition, high pore-fluid pressures would promote failure on pre-existing weaknesses by reducing normal stresses. The most likely volatile species to be exsolved from basaltic magmas in deep crustal sills is carbon dioxide (CO_2) [*Holloway & Blank*, 1994]. Although water, sulphur dioxide and other volatiles are likely to be present in basaltic magmas, they are at lower concentrations (less than 1 wt%, or 10,000 ppm [e.g. *Hartley et al*., 2014]). More importantly for our present discussion, the strong pressure dependence of CO_2 solubility means that CO_2 exsolves at

greater depths than water and sulphur, which remain dissolved in the magma until much shallower depths (< 1 km). In contrast, CO_2 may start to exsolve from rising magmas at depths of tens of kilometres (depending on the bulk CO_2 content of the magma) as the melt decompresses and becomes supersaturated [*Pan et al.* 1991*; Lowenstern,* 2001]. So as melt intrudes upward and decompresses, it exsolves a fluid rich in CO_2, with further volatile exsolution continuing as the melt fractionates [*Turner et al.*, 2012]. At high pressures in the crust, this fluid will be supercritical; at low pressures the fluid becomes an exsolved vapour phase. A CO_2-rich volatile-phase exsolved from intruding mafic magmas has also been suggested as the trigger of swarms of earthquakes imaged beneath Mammoth Lakes in the USA [*Shelly & Hill,* 2011], an area where high CO_2 fluxes are also observed at the surface.

Carbon dioxide concentrations measured in ocean island basalts are variable. Melt inclusions hosted by olivine in tholeiitic basalts erupted from Kilauea, Hawai'i contain up to 800 ppm [*Sides et al.,* 2014]; from the Azores and Canary Islands up to 4000 ppm [*Metrich et al*., 2014; *Longpre et al.*, 2017] and in Iceland, up to 1200 ppm [*Maclennan*, 2017]. However, it is difficult to constrain 'primary' concentrations in the melt because volatiles may be lost before the magma freezes, so these may be unreliable measurements of the original concentrations. In addition, CO_2 may be sequestered into a shrinkage bubble [*Hartley et al*., 2014; *Sides et al*., 2014b; *Wallace et al.,* 2015] or lost due to decrepitation [*Maclennan*, 2017]. One approach to get round this problem is to examine depleted melts (preserved as melt inclusions or as quenched matrix glass on the sea floor) from oceanic basalt samples which have not undergone degassing.

It is thought that CO_2 behaves similarly to Nb and Ba on melting [*Rosenthal et al.,* 2015] and so the CO_2/Nb and CO_2/Ba ratios of these undegassed melts may provide a way to reconstruct primary melt CO_2 contents, given the Nb concentration. Samples of these kinds of depleted melts are relatively rare. For glasses from the Siqueros Fracture Zone, the CO_2/Nb ratio is 239 ± 46 [Saal *et al.,* 2002] and the CO_2/Nb ratio of olivine-hosted melt inclusions from Borgarhraun, Iceland, are 391 ± 16 [*Hauri et al*., 2018]. The CO_2/Nb ratio may correlate with other proxies for mantle heterogeneity such as Nd isotopic composition [*Hauri et al*., 2018]. Most olivine-hosted melt inclusions from Iceland show signs of pre-entrapment degassing, CO_2 sequestration into a bubble and/or decrepitation (see review by *Maclennan*, 2017), but the Nb concentrations of primitive melts may be used to place bounds on primary melt CO_2 concentrations. Using the range in Nb concentrations in depleted and enriched melts in central Iceland [*Hartley et al.,* 2014, 2017*; Hauri et al.,* 2018], we estimate that primitive melts ascending from Moho depths beneath central Iceland may contain between 800 to 4800 ppm CO_2. The carbon solubility model of Eguchi & Dasgupta (2018) indicates that melts containing this amount of CO_2 will become saturated in a CO_2-rich exsolved fluid phase at 0.12 to 0.7 GPa (~ 5 to 25 km depth).

Prolonged storage and fractionation of basaltic melts in lenses at depths similar to, or less than these depths may yield segregation of the CO_2-rich fluid. In cooling and fractionating sills of thickness 10 metres, for example, bubbles of 1 mm size take of the order of $10^6 - 10^7$ seconds for segregation of foam to occur (for gas volume fractions of 0.5 to 1.0 %, with a melt viscosity of 100 Pa s and a density of 2700 kg m^{-3}) [*Menand and Phillips*, 2007]. A gas volume fraction of 0.5 − 1 vol% CO_2 at a depth of ~ 10 km requires an exsolved CO_2 fraction of 1000 to 3000 ppm (from the Ideal Gas Law and using a melt density of 2700 kg m^{-3}), which is consistent with estimates of the bulk magma CO_2 content noted above and the expected exsolved fraction at that depth [*Hartley et al*., 2014]. It is worth noting that higher viscosity magmas would freeze before they can segregate their exsolved volatiles to the roof of the sill and therefore this process is particularly relevant for low viscosity basalts in ocean island settings. Once segregated at the roof of the sill, the CO_2 may migrate into the overlying

crust and elevate pore fluid pressures, which may induce brittle failure of the crust and earthquakes, as has been observed at Mammoth, USA [*Hill et al.*, 2006], Matsushiro, central Japan [*Cappa et al.*, 2009] and Askja [*Greenfield & White*, 2015]. The emissions of CO_2 in Iceland that precede eruptions have so far proven difficult to observe directly. Magmatic CO_2 may be sequestered into shallow, geothermally heated, convecting groundwater cells, or directly into meltwater at the base of the ice sheets, or in calcite precipitation. Efforts to understand the fate of magmatic CO_2 in Icelandic systems are ongoing [e.g. *Barry et al.*, 2014].

Conclusions

Iceland provides a superb natural laboratory for investigating melt plumbing: there is a high rate of production of melt, which means that there is a lot of melt within and erupted from the crust; the tectonic setting is relatively simple, with rift zones crossing a mantle plume; background seismic noise is low, which allows tiny earthquakes deep within the crust to be detected and mapped; and the relatively young age of the basaltic rocks means that largely unaltered petrologic samples can be obtained and analysed. We show a variety of examples of melt intruding the crust and stalling in sills at all depths from the upper mantle just below the Moho, through the crust, and in large storage regions at shallow depths under the central volcanoes. The combination of geochemical barometers on the matrix and crystals entrained within erupted basalts, together with direct measurements from small earthquakes of the depths at which melt is moving today in the crust provide complementary information on the history of the melt as it works towards the surface from it's deep mantle source. It is well known that volatiles play a crucial role in driving eruptions at shallow levels beneath volcanoes: we suggest here that the exsolution of CO_2 from basalts at lower- to mid-crustal levels plays an equally important role in facilitating the movement of melt towards the surface through a sequence of intermediate sills in each of which fractionation can proceed.

References

Ágústsdóttir, T., Woods, J., Greenfield, T., Green, R. G., White, R. S., Winder, T., Brandsdóttir, B., Steinthórsson, S. & Soosalu, H. 2016 Strike-slip faulting during the 2014 Bárðarbunga-Holuhraun dike Intrusion, central Iceland. *Geophys. Res. Lett*, plus Supplementary Information, **43**, 1495–1503 (DOI 10.1002/2015GL067423).

Alfaro, R., Brandsdóttir, B., Rowlands, D. P., White, R. S. & Gudmundsson, M. T. 2007 Structure of the Grímsvötn central volcano under the Vatnajökull icecap, Iceland, *Geophys. J. Int.*, **168**, 863–876 (DOI 10.1111/j.1365-246X.2006.03238.x)

Bali, E., Hartley, M. E., Halldorsson, S. A., Gudfinnsson, G. H. & Jakobsson, S. 2018 Melt inclusion constraints on volatile systematics and degassing history of the 2014-2015 Holuhraun eruption, Iceland, *Cont. Miner. Petr.* **173(2)** (DOI 10.1007/s00410-017-1434-1).

Barry, P. H., Hilton, D. R., Füri, E., Halldórsson, S. A. & Grönvold, K. 2014 Carbon isotope and abundance systematics of Icelandic geothermal gases, fluids and subglacial basalts with implications for mantle plume-related CO_2 fluxes, *Geochim. Cosm. Acta.*, **134**, 74–79, (DOI 10.1016/j.gca.2014.02.038)

Bell, A. F. & C. R. J. Kilburn 2012 Precursors to dyke-fed eruptions at basaltic volcanoes: insights from patterns of volcano-tectonic seismicity at Kilauea volcano, Hawaii, *Bull. Volcanol.*, **74**, 325–339, (DOI 10.1007/s00445-011-0519-3).

Brandsdóttir, B. & Menke, W. H. 1992 Thin low-velocity zone within the Krafla caldera, NE-Iceland attributed to a small magma chamber. *Geophys. Res. Lett.*, **19**, 2381–2384.

Brandsdóttir, B., Menke, W., Einarsson, P., White, R. S. & Staples, R. K. 1997 Färoe-Iceland Ridge Experiment, 2. Crustal structure of the Krafla central volcano. *J. Geophys. Res.*, **102**, 7867–7886.

Cappa, F., Rutqvist, J., Yamamoto, K., 2009. Modeling crustal deformation and rupture processes related to upwelling of deep CO2-rich fluids during the 1965–1967 Matsushiro earthquake swarm in Japan. *J.Geophys. Res. Solid Earth*, **114** (DOI 10.1029/2009JB006398)

Chanceaux, L. & Menand, T. 2014 Solidification effects on sill formation: an experimental approach, *Earth Planet. Sci. Lett.*, **403**, 79–88, (DOI 10.1016/j.epsl.2014.06.018).

Cmíral, M., Fitz Gerald, J. D., Faul, U. H. & Green, D. H. 1998 A close look at dihedral angles and melt geometry in olivine-basalt aggregates: a TEM study, *Contrib. Mineral. Petrol.*, **130**, 336–345.

Darbyshire, F.A., Bjarnason, I.T., White, R.S. & Flóvenz, Ó.G., 1998. Crustal structure above the Iceland mantle plume imaged by the ICEMELT refraction profile. *Geophys. J. Int.*, **135**, 1131−1149.

Darbyshire, F. A., White, R. S. & Priestley, K. P. 2000. Structure of the crust and uppermost mantle of Iceland from a combined seismic and gravity study. *Earth Planet. Sci. Lett.*, **181**, 409–428.

DeMets C., Gordon, R. G. & Argus, D. F. 2010 Geologically current plate motions. *Geophys. J. Int.*, **181**, 1–80.

Eguchi, J. & Dasgupta, R. 2018. A CO_2 solubility model for silicate melts from fluid saturation to graphite or diamond saturation, *Chem. Geol.*, **487**, 23–38 (DOI 10.1016/j.chemgeo.2018.04.012)

de Zeeuw-van Dalfsen, E., H. Rymer, H., Sturkell, E., Pedersen, R., Hooper, A., Sigmundsson, F. & Ófeigsson, B. G. 2013. Geodetic data shed light on ongoing caldera subsidence at Askja, Iceland, *Bull. Volcanol.*, **75(5)**, 709 (DOI 10.1007/s00445-013-0709-2).

Einarsson P. 2018 Short-term seismic precursors to Icelandic eruptions 1973-2014, *Front. Earth Sci.*, **6**, (DOI 10.3389/feart.2018.00045)

Einarsson P. 1978 S-wave shadows in the Krafla Caldera in NE-Iceland, evidence for a magma chamber in the crust. *Bull. Volcanol.*, **41**, 187–195.

Einarsson, P. & Brandsdóttir, B. 1978 Seismological evidence for lateral magma intrusion during the July 1978 deflation of the Krafla volcano in NE-Iceland, *J. Geophys.*, **47**, 160–165.

Einarsson, P. & Sæmundsson, K. 1987 Earthquake epicenters 1982-1985 and volcanic systems in Iceland (Map). (Menningarsjóður, Reykjavík, 1987).

Einarsson, P., Brandsdóttir, B., Gudmundsson, M. T., Björnsson, H., Grönvold, K., & Sigmundsson, F. 1997 Center of the Iceland hotspot experiences volcanic unrest. *Eos, Trans. Amer. Geophys. Union*, **78(35)**, 369–375.

French, S. W. & Romanowicz, B. 2015 Broad plumes rooted at the base of the Earth's mantle beneath major hot spots. *Nature*, **525**, 95–99.

Greenfield, T., & White, R. S. 2015 Building Icelandic igneous crust by repeated melt injections, *J. Geophys. Res. Solid Earth*, **120**, 7771–7788, (DOI 10.1002/2015JB012009).

Greenfield, T., White, R. S. & Roecker, S. 2016 The magmatic plumbing system of the Askja central volcano, Iceland as imaged by seismic tomography, *J. Geophys. Res., Solid Earth* **121**, 7211–7229 (DOI 10.1002/2016JB013163).

Greenfield, T., White, R. S., Winder, T. & Ágústsdóttir, T. 2018 Seismicity of the Askja and Bárðarbunga volcanic systems of Iceland, 2009–2015, *J. Volc. Geotherm. Res.*, in press.

Gronvold, K., Halldorsson, S. A., Sugurdsson, G. Sverrisdottir, G. & Óskarsson, N. 2008 Isotopic systematics of magma movement in the Krafla central volcano, north Iceland, in *Geochim. Cosm. Acta Supplement, Goldschmidt Conference Abstracts*, **72**, p. 331.

Gudmundsson, O., Brandsdóttir, B., Menke, W. & Sigvaldason, G. E. 1994 The crustal magma chamber of the Katla volcano in south Iceland revealed by 2-D seismic undershooting. *Geophys. J. Int.*, **119,** 277–296.

Halldórsson S. A., Bali, E., Hartley M., Neave, D., Peate, D., Gudfinnsson, G., Bindeman I., Whitehouse M., Riishus, M., Pedersen, G. et al., 2018, Petrology and geochemistry of the 2014-2015 Holuhraun eruption, central Iceland: compositional and mineralogical characteristics, temporal variability and magma storage. *Contr. Min. Petr.*, (DOI 10.1007/s00410-018-1487-9).

Hardarson, B. S., Fitton, J. G., Ellam, R. M. & Pringle, M. S., 1997 Rift relocation - A geochemical and geochronological investigation of a palaeo-rift in northwest Iceland. *Earth Planet Sci. Lett.* **153**, 181–196.

Hartley, M. E. & Thordarson, T. 2012 The 1874-1876 volcano-tectonic episode at Askja, North Iceland: Lateral flow revisited, *Geochem. Geophys. Geosys.*, **14(7),** 2286–2309 (DOI 10.1002/ggge.20151).

Hartley, M. E., Maclennan, J., Edmonds, M. & Thordarson, T., 2014 Reconstructing the deep CO_2 degassing behaviour of large basaltic fissure eruptions. *Earth Planet. Sci. Letts.*, **393**, 120–131.

Hartley, M. E., Bali, E., Maclennan, J., Neave, D. A. & Halldórsson, S.A. 2018 Melt inclusion constraints on petrogenesis of the 2014–2015 Holuhraun eruption, Iceland. *Contr. Min. Pet.*, **173(2),** 10–33. (DOI 10.1007/s00410-017-1435-0)

Hauri, E. H., Maclennan, J., McKenzie, D., Gronvold, K., Oskarsson, N. & Shimizu, N., 2018. CO2 content beneath northern Iceland and the variability of mantle carbon. *Geology* **46**, 55–58.

Hawkesworth, C., Blake, S., Evans, P., Hughes, R., Macdonald, R., Thomas, L., Turner, S., & Zellmer, G., 2000 Time scales of crystal fractionation in magma chambers—integrating physical, isotopic and geochemical perspectives: *J. Pet.*, **41**, 991–1006.

Helz, R. T., Clague, D. A., Mastin, L. G. & Rose, T. R., 2015. Evidence for large compositional ranges in coeval melts erupted from Kīlauea's summit reservoir. In: *Hawaiian Volcanoes: From Source to Surface, Geophysical Monograph* **208**, 125–145.

Hjartardóttir, A. R., Einarsson, P., & Sigurdsson, H. 2009 The fissure swarm of the Askja volcanic system along the divergent plate boundary of N Iceland. *Bull.Volcanol.* **71,** 961–975.

Hjartardóttir, A. R., & Einarsson, P. 2012 The Kverkfjöll fissure swarm and eastern boundary of the Northern Volcanic Rift Zone, Iceland. *Bull.Volcanol.* **74,** 143–162.

Hjaltardóttir, S., Vogfjord, K. S. & Slunga, R., 2009 Seismic signs of magma pathways through the crust in the Eyjafjallajökull volcano, South Iceland, *Icelandic Meteorological Office Report*, VI 2009–013, Reykjavik.

Holloway, J. R. & Blank, J. G., 1994 Application of experimental results to C-O-H species in natural melts, *Reviews in Mineralogy*, **30**, 187–230.

Hooper, A., Ófeigsson, B., Sigmundsson, F., Lund, B., Einarsson, P., Geirsson, H. & Sturkell, E., 2011 Increased capture of magma in the crust promoted by ice-cap retreat in Iceland. *Nature Geoscience*, **4**, 783–786 (DOI 10.1038/ngeo1269).

Hudson, T. S., White, R. S., Greenfield, T., Ágústsdóttir, T., Brisbourne, A. & Green, R. G. 2017 Deep crustal melt plumbing of Bárðarbunga volcano, Iceland, *Geophys. Res. Lett.*, **44**, 8785–8794, (DOI 10.1002/2017GL074749)

Jenkins, J. S., Cottaar, S., White, R. S. & Deuss, A. 2016 Depressed mantle discontinuities beneath Iceland: Evidence of a garnet controlled 660 km discontinuity? *Earth Planet. Sci. Lett.*, **433**, 159–168 (DOI 10.1016/j.epsl.2015.10.053).

Jenkins, J., Maclennan, J., Green, R. G., Cottaar, C. & White, R. S. 2018 Crustal formation on a spreading ridge above a mantle plume: receiver function imaging of the Icelandic crust, *J. Geophys. Res., Solid Earth* (DOI 10.1029/2017JB015121).

Kavanagh, J. L., Menand, T. & Sparks, R. S. J., 2006 An experimental investigation of sill formation and propagation in layered elastic media, *Earth Planet. Sci. Lett.*, **245**, 799–813, (DOI 10.1016/j.epsl.2006.03.025).

Kavanagh, J. L. & Sparks, R. S. J., 2011. Insights of dyke emplacement mechanics from detailed 3-D dyke thickness datasets. *J. Geol. Soc. Lond.* (DOI 10.1144/0016-76492010-137).

Keiding, J. K. & Sigmarsson, O., 2012 Geothermobarometry of the 2010 Eyjafjallajökull eruption: New constraints on Icelandic magma plumbing systems, *J. Geophys. Res.*, **117**, B00C09 (DOI 10.1029/2011JB008829).

Kelemen, P., Koga, K. & Shimizu, N. 1997 Geochemistry of gabbro sills in the crust-mantle transition zone of the Oman ophiolite: Implications for the origin of the oceanic lower crust. *Earth Planet. Sci. Lett.*, **146,** 475–488 (DOI 10.1016/S0012-821X(96)00235-X).

Kiser, E., Palomeras, I., Levander, A., Zelt, C., Harder, S., Schmandt, B., Hansen, S., Creager, K., & Ulberg, C. 2016 Magma reservoirs from the upper crust to the Moho inferred from high-resolution Vp and Vs models beneath Mount St. Helens, Washington State, USA. *Geology*, **44**, 411–414.

Klügel, A., Longpré, M.-A., García-Cañada, L. & Stix, J. 2015 Deep intrusions, lateral magma transport and related uplift at ocean island volcanoes, *Earth Planet. Sci. Lett.*, **431**, 140–149, (DOI 10.1016/j.epsl.2015.09.031).

Kokfelt, T.F., Hoernle, K.A.J., Hauff, F., Fiebig, J., Werner, R. & Garbe-Schonberg, D., 2006 Combined trace element and Pb-Nd–Sr-O isotope evidence for recycled oceanic crust (upper and lower) in the Iceland mantle plume, *J. Pet.*, **47**, 1705–1749 (DOI 10.1093/petrology/egl025).

Laumonier, M., Farla, R., Frost, D. J., Katsura, T., Marquardt, K., Bouvier, A. S. & Baumgartner, L. P. 2017 Experimental determination of melt interconnectivity and electrical conductivity in the upper mantle, *Earth Planet. Sci. Lett.*, **463**, 286–297 (DOI 10.1016/j.epsl.2017.01.037).

Lin, G. & Okubo, P. G. 2016 A large refined catalog of earthquake relocations and focal mechanisms for the Island of Hawai'i and its seismotectonic implications, *J. Geophys. Res. Solid Earth*, **121**, 5031–5048 (DOI 10.1002/2016JB013042).

Longpré M. A., Stix J., Klügel A. & Shimizu N. 2017 Mantle to surface degassing of carbon-and sulphur-rich alkaline magma at El Hierro, Canary Islands. *Earth Planet. Sci. Lett.*, **460**, 268 – 280.

Lowenstern, J. B. 2001 Carbon dioxide in magmas and implications for hydrothermal systems, *Mineralium Deposita*, **26**, 490–502

Maclennan, J., McKenzie, D. & Gronvöld, K. 2001a Plume-driven upwelling under central Iceland, *Earth Planet. Sci. Lett.*, **194,** 67–82 (DOI 10.1016/S0012-821X(01)00553-2)

Maclennan, J., McKenzie, D., Gronvöld, K. & Slater, L. 2001b Crustal accretion under northern Iceland, *Earth Planet. Sci. Lett.*, **191(3),** 295–310.

Maclennan, J. 2017 Bubble formation and decrepitation control the CO2 content of olivine-hosted melt inclusions. *Geochem., Geophys., Geosys.*, **18**, 597–616 (DOI 10.1002/2016GC006633).

Martens, H. R. & White, R. S. 2013 Triggering of microearthquakes in Iceland by volatiles released from a dyke intrusion, *Geophys. J. Int.*, **194,** 1738–1754, (DOI 10.1093/gji/ggt184).

Menand, T. 2011 Physical controls and depth of emplacement of igneous bodies: A review, *Tectonophys.*, **500**, 11–19, (DOI 10.1016/j.tecto.2009.10.016).

Menand, T. & Phillips, J. C. 2007 Gas segregation in dykes and sills. *Journal of Volcanology and Geothermal Research*, **159,** 393–408.

Métrich, N., Zanon, V., Créon, L., Hildenbrand, A., Moreira, M. & Marques, F. O. 2014 Is the 'Azores hotspot' a wetspot? Insights from the geochemistry of fluid and melt inclusions in olivine of Pico basalts. *J. Petrology*, **55(2)** 377−393.

Neave, D. A., & Putirka, K. D. 2017 A new clinopyroxene-liquid barometer, and implications for magma storage pressures under Icelandic rift zones, *Amer. Mineralogist* **102**, 777–794.

Okubo, P. G. & Wolfe, C. J. 2008 Swarms of similar long-period earthquakes in the mantle beneath Mauna Loa Volcano, *J. Volc. Geotherm. Res.*, **178**, 787–794. (DOI: 10.1016/j.jvolgeores.2008.09.007).

Pálmason, G., 1971 Crustal structure of Iceland from explosion seismology. *Soc. Sci. Islandica.* (DOI:10.7185/geochemlet.1509)

Pan, V., Holloway, J. R. & Hervig, R. L. 1991. The pressure and temperature dependence of carbon dioxide solubility in tholeiitic basalt melts, *Geochem. Cosmochim. Acta.,* **55**, 1587–1595.

Pitt, A. M., Hill, D. P., Walter, S. W. & Johnson, M. J. S., 2002 Midcrustal, long-period earthquakes beneath northern California volcanic areas, *Seism. Res. Lett.,* **73**, 144–152.

Martens, H. R. & White, R. S. 2013 Triggering of microearthquakes in Iceland by volatiles released from a dyke intrusion, *Geophys. J. Int.*, **194 (3),** 1738–1754. (DOI 10.1093/gji/ggt184).

Rubin, A. M. & Gillard, D. 1998 Dike-induced earthquakes: Theoretical considerations, *J. Geophys. Res. Solid Earth*, **103**, 10,017–10,030 (DOI 10.1029/97JB03514).

Saal, A.E., Hauri, E.H., Langmuir, C.H. & Perfit, M.R., 2002 Vapour undersaturation in primitive mid-ocean-ridge basalt and the volatile content of Earth's upper mantle, *Nature*, **419**, 451–455.

Schuler, J., Greenfield, T., White, R.S., Roecker, S. W., Brandsdóttir, B., Stock, J. M., Tarasewicz, J., Martens, H. & Pugh, D. 2015 Seismic imaging of the shallow crust beneath the Krafla central volcano, NE Iceland, *J. Geophys. Res.*, **120**, 7156−7173, (DOI 10.1002/2015JB012350).

Shelly, D. R. & Hill, D. P. 2011 Migrating swarms of brittle-failure earthquakes in the lower crust beneath Mammoth Mountain, California, *Geophys. Res. Lett., **38*(20)**, 1–6. (DOI 10.1029/2011GL049336).

Sides, I.R., Edmonds, M., Maclennan, J., Swanson, D.A., Houghton, B.F., 2014. Eruption style at Kīlauea Volcano in Hawai`i linked to primary melt composition *Nat. Geosci.* **7**, 464–469.

Sigmarsson, O., Vlastelic, I., Andreasen, R., Bindeman, I., Devidal, J.-L., Moune, S., Keiding, J. K., Larsen, G., Höskuldsson, A. & Thordarson, Th. 2011, Remobilization of silicic intrusion by mafic magmas during the 2010 Eyjafjallajökull eruption, *Solid Earth*, **2**, 271–281 (DOI 10.5194/se-2-271-2011).

Sigmundsson, F., Hreinsdóttir, S., Hooper, A., Arnadóttir, T., Pedersen, R., Roberts, M.J., Óskarsson, N., Auriac, A., Decriem, J., Einarsson, P. and Geirsson, H., 2010. Intrusion triggering of the 2010 Eyjafjallajökull explosive eruption. *Nature*, **468**, 426–430, doi:10.1038/nature09558

Sigmundsson, F., Hooper, A., Hreinsdóttir, S., Vogfjord, K., Ófeigsson, B., Heimisson, E. R., Dumont, S., Parks, M., Spaans, K., Guðmundsson, G. B., et al. 2015 Segmented lateral dyke growth in a rifting event at Bárðarbunga volcanic system, Iceland, *Nature*, **517**, 191–195. (DOI 10.1038/nature14111).

Sigurdsson, H. & Sparks, R. S. J. 1978 Lateral magma flow within rifted Icelandic crust. *Nature* **274**, 126–130

Stroncik, N. A., Klügel, A. & Hansteen, T. H. 2009 The magmatic plumbing system beneath El Hierro (Canary Islands): constraints from phenocrysts and naturally quenched basaltic glasses in submarine rocks. *Contrib. Min. Pet.*,**157,** 593–607 (DOI 10.1007/s00410-008-0354-5)

Tarasewicz, J., White, R. S., Woods, A. W., Brandsdóttir, B. & Gudmundsson, M. T. 2012 Magma mobilization by downward-propagating decompression of the Eyjafjallajökull volcanic plumbing system, *Geophys. Res. Lett.*, **39**, L19309. (DOI 10.1029/2012GL053518).

Tarasewicz, J., White, R. S. & Brandsdóttir, B. 2014, Seismogenic magma intrusion before the 2010 eruption of Eyjafjallajökull volcano, Iceland, *Geophys. J. Int.*, **198**, 906–921, plus supplementary information (DOI 10.1093/gji/ggu169).

Thorarinsson, S. 1962 The eruption in Askja, 1961 A preliminary report, *Am. J. Sci.*, **260**, 641–651.

Turner, S., Reagan, M., Vigier, N. & Bourdon, B. 2012 Origins of ^{210}Pb-^{226}Ra disequilibria in basalts: New insights from the 1978 Asal Rift eruption, *Geochem., Geophys., Geosyst.*, **13**, (DOI 10.1029/2012GC004173).

Vinet, N. & Higgins, M. D. 2010 Magma solidification processes beneath Kilauea volcano, Hawaii: A quantitative textural and geochemical study of the 1969-1974 Mauna Ulu Lavas, *J. Petrol.*, **51**, 1297–1332 (DOI 10.1093/petrology/egq020).

von Seggern, D. H., Smith, K. D. & Preston, L. A. 2008 Seismic spatial-temporal character and effects of a deep (25–30 km) magma intrusion below North Lake Tahoe, California-Nevada, *Bull. Seismol. Soc. Am.*, **98**, 1508–1526 (DOI: 10.1785/0120060240)

Wallace, P. J., Kamenetsky, V. S. & Cervantes, P. Melt inclusion CO2 contents, pressures of olivine crystallization, and the problem of shrinkage bubbles. *American Mineralogist*, **100(4),** 787–794 (DOI 10.2138/am-2015-5029)

Wech, A. G., & Thelen, W. A. 2015 Linking magma transport structures at Kilauea volcano, *Geophys. Res. Lett.*, **42**, 7090–7097 (DOI 10.1002/2015GL064869).

White, R., & McCausland, W. 2016 Volcano-tectonic earthquakes: A new tool for estimating intrusive volumes and forecasting eruptions, *J. Volcanol. Geotherm. Res.*, **309,** 139–155, (DOI 10.1016/j.jvolgeores.2015.10.020).

White, R. S., McKenzie, D. & O'Nions, R. K. 1992 Oceanic crustal thickness from seismic measurements and rare earth element inversions. *J. Geophys. Res.*, **97**, 19,683–19,715.

White, R. S., Drew, J., Martens, H. R. Key, J., Soosalu, H. & Jakobsdóttir, S. S. 2011 Dynamics of dyke intrusion in the mid-crust of Iceland, *Earth Planet. Sci. Lett.*, **304**, 300–312, (DOI 10.1016/j.epsl.2011.02.038).

White, R. S., Redfern, S. A. T. & Chien, S.-Y. 2012 Episodicity of seismicity accompanying melt intrusion into the crust, *Geophys. Res. Lett.*, **39**, L08306, (DOI 10.1029/2012GL051392).

Woods, J., Donaldson, C., White, R. S., Brandsdóttir, B., Caudron, C., Hudson, T. S. & Ágústsdóttir, T. 2018 Long-period seismicity reveals magma pathways above a propagating dyke during the 2014–15 Bárðarbunga rifting episode, Iceland, *Earth Planet. Sci. Lett.*, **490**, 216–219 (DOI 10.1016/j.epsl.2018.03.020)

Wright, T. L. & Klein, F. W. 2006 Deep magma transport at Kilauea volcano, Hawaii, *Lithos*, **87**, 50–79 (DOI 10.1016/j.lithos.2005.05.004).

Yang, H.-J., Kinzler, R. J. & Grove, T.L. 1996 Experiments and models of anhydrous, basaltic olivine-plagioclase-augite saturated melts from 0.001 to 10 kbar. *Contrib. Miner. Petrol.* **124**, 1–18.

Zhu, W., Gaetani, G. A., Fusseis, F., Montési, L. G. & De Carlo, F., 2011. Microtomography of partially molten rocks: three-dimensional melt distribution in mantle peridotite. *Science* **332**, 88–91.

Acknowledgments

We are grateful to several generations of graduate students who have contributed both by fieldwork and in data processing and analysis to the results presented here. Seismometers were provided by the Natural Environmental Research Council SEIS-UK under loans 842, 857, 914, 968, 980 and 1022, and the Icelandic Meteorological Office kindly provided data from some of their seismometers. We thank all those who gathered the seismic data from the field, in particular Sveinbjörn Steinþórsson and Bryndís Brandsdóttir from the Institute of Earth Sciences, University of Iceland. Jeff Karson kindly provided helpful comments on the manuscript. Department of Earth Sciences, Cambridge contribution number esc.4310.

Funding Statement
Funding was provided to RSW by Natural Environment Research Council grants NE/F011407/1, NE/H025006/1 and NE/M017427/1, and the European Community's Seventh Framework Programme grant 308377 (Project FUTUREVOLC).

Competing Interests
The authors have no competing interests.

Authors' Contributions
The first draft was written by Robert White, and all authors added material and approved the final version.